Paper:

Performance-Based Tsunami Engineering via a Web-Based GIS Data Explorer

Dylan Keon[*,†], **Cherri M. Pancake**[**], **Ben Steinberg**[*], **and Harry Yeh**[***]

[*]Northwest Alliance for Computational Science and Engineering, Oregon State University
2007 Kelley Engineering Center, Oregon State University, Corvallis, OR 97331, USA
[†]Corresponding author, E-mail: dylan.keon@oregonstate.edu
[**]School of Electrical Engineering and Computer Science, Oregon State University, USA
[***]School of Civil and Construction Engineering, Oregon State University, USA

In spite of advances in numerical modeling and computer power, coastal buildings and infrastructures are still designed and evaluated for tsunami hazards based on parametric criteria with engineering "conservatism," largely because complex numerical simulations require time and resources in order to obtain adequate results with sufficient resolution. This is especially challenging when conducting multiple scenarios across a variety of probabilistic occurrences of tsunamis. Numerical computations that have high temporal and spatial resolution also yield extremely large datasets, which are necessary for quantifying uncertainties associated with tsunami hazard evaluation. Here, we introduce a new web-based tool, the Data Explorer, which facilitates the exploration and extraction of numerical tsunami simulation data. The underlying concepts are not new, but the Data Explorer is unique in its ability to retrieve time series data from massive output datasets in less than a second, the fact that it runs in a standard web browser, and its user-centric approach. To demonstrate the tool's performance and utility, two examples of hypothetical cases are presented. Its usability, together with essentially instantaneous retrieval of data, makes simulation-based analysis and subsequent quantification of uncertainties accessible, enabling a path to future design decisions based on science, rather than relying solely on expert judgment.

Keywords: tsunami, web-based, GIS, prediction, sensitivity analysis

1. Introduction

The 2011 East Japan Tsunami caused enormous economic damage. One of the most striking and unprecedented effects of the 2011 tsunami was the failure of sturdy reinforced concrete buildings and coastal protection structures such as seawalls, coastal dikes, and breakwaters, some of which had been designed and constructed specifically for tsunami protection [1, 2]. During the tsunami, some of the "tsunami-resistant" build-

ings in coastal areas were unexpectedly destroyed and/or completely inundated, resulting in multiple casualties [3–5]. Most notably, the failure of the Fukushima Dai-Ichi Nuclear Power Plant released radioactive contamination, forcing the abandonment of cities and towns. Even after five years, the radioactive contamination has not been controlled, and decommissioning the reactors is expected to cost at least $15 billion [6]. The 2011 tsunami clearly demonstrated the importance of protecting critical coastal structures such as bridges, oil and LNG storage facilities, nuclear and fossil fuel power plants, military and civilian ports, schools and hospitals, and buildings used for vertical evacuation.

The accelerating rate of construction of critical infrastructure in coastal zones requires a better understanding of design methodology for tsunami-resistant structures. To analyze the performance of buildings and infrastructures in a tsunami scenario, it is necessary to know not only the maximum runup heights and inundation zone, but also the time histories of flow depth and velocities at a location of interest within the inundation zone in order to evaluate tsunami-induced forces, moments, soil instabilities, and buoyancy forces [7]. Time series data required for analysis of buildings and infrastructures are much more difficult to compute than the relatively straightforward determination of maximum inundation limit, further complicating the process and often necessitating high performance computing resources [8]. It is also important to note that, because critical structures require cost-benefit analysis, tsunami hazard prediction at the site of interest should be based on probabilistic analyses that clearly identify uncertainties.

Many sources of uncertainty complicate the proper quantification of tsunami hazards. All probabilistic estimates of tsunami hazard are based on the probability distribution of possible tsunamigenic earthquakes that are not well defined, due to the lack of real event populations (i.e., measured data) and unreliable imaginary experiments (i.e., artificially-created data). As such, the probability space itself is inadequate and uncertain. The present state of probabilistic tsunami hazard assessment represents an attempt to achieve the best estimate by expert judgment, based on available science and data. Even

Fig. 1. Tsunami destruction pattern in the town of Onagawa, Japan: (left – before the 2011 Tsunami [source: Google Earth]; right – after the event [source: Satake]). A pair of sturdy buildings at the waterfront acted as barriers for the buildings behind. The gap between the buildings created a swift jet flow, wiping out everything in the flow path.

if all tsunamigenic earthquake sources were to be identified, other factors may still create uncertainty: (1) initial tsunami formations, (2) tsunami propagation, transformation, and interaction with the continental shelves and nearshore topography, and (3) tsunami inundation/drawdown processes influenced by topography, manmade structures, and infrastructures (roads, coastal protective structures, canals, etc.).

Figure 1 displays the state of the town of Onagawa, Japan, before and after the 2011 tsunami. The damage pattern indicates that a pair of sturdy waterfront buildings acted as a barrier for smaller buildings behind them (the smaller buildings were in the "tsunami shadow" of the larger buildings). This spatial arrangement resulted in a strong flow jet formation in the gap between the two large buildings. The resulting complete destruction of buildings in the path of the jet formation can be observed in the figure. Obviously, the maximum inundation depths and zones indicated in tsunami inundation maps of this area contain substantial uncertainty. Because of substantial spatial variability in tsunami effects, engineering analysis should be performed with careful consideration of the flow conditions not only at the site itself but also for a certain area surrounding the site.

Even if a probabilistic tsunami loading can be determined for engineering purposes, the structural response imposes an additional dimension of uncertainty. A tsunami can induce multiple factors that cause structural failures, such as destructive fluid forces, debris impact and jamming forces, fires, and soil liquefaction and foundation scouring. The uncertainty of human response in an evacuation scenario only complicates the hazard and risk assessment [9]. Considering the substantial uncertainties involved in the estimation of tsunami hazards and concomitant structural responses, a scenario-based and

performance-based approach is necessary.

Our understanding of tsunami behavior has advanced considerably since the 1960 Chile tsunami event [10]. In particular, capabilities for modeling and monitoring tsunamis have improved significantly in recent years. Despite these advances in knowledge and understanding, however, uncertainty remains a key challenge in the determination of tsunami hazards. This paper presents a demonstration of data-driven capabilities that can be used to evaluate a tsunami's effects on structures and facilities.

2. Current Practice

Efforts have been made recently toward the development of probabilistic estimates of tsunami hazard, often called "probabilistic tsunami hazard assessment" (PTHA) [11–15]. PTHA methods are built upon a long-implemented method used for probabilistic earthquake ground motion, called probabilistic seismic hazard assessment (PSHA) [16, 17], and take into consideration all of the possible tsunami sources that might affect a site of interest. First, seismic parameters at the potential tsunami sources are specified, then a probability model (often the Poisson model) is chosen that estimates the occurrence of the event over time. Based on stochastic tsunami sources, a hydrodynamic numerical model for each source location and parameter is run to compute tsunami propagation and the consequential tsunami hazard at a site of interest. Finally, the model results are aggregated, thereby incorporating uncertainty.

Uncertainty estimates are categorized into two classes: epistemic and aleatory. Epistemic uncertainty represents our knowledge related to geophysical problems (e.g., the prediction of earthquake processes); this is incorporated via the use of logic trees based on expert opinion and judgment together with empirical data, if available. Aleatory uncertainty relates to the variability of processes, incorporated in mathematical problems that deal with a probability distribution modeling the uncertainty. The end products are probabilistic estimates (often in the form of hazard curves) of the scalar parameters (i.e., maximum tsunami heights).

At present, probabilistic tsunami hazard is identified only by maximum tsunami wave height and/or inundation depth [14, 18]. Tsunami flow velocities and forces are computed based on those heights and depths. Some attempts have been made to develop methodologies to compute tsunami loadings on structures [19] and to develop fragility curves for buildings [20, 21]. FEMA P646 [19] presents a methodology to estimate tsunami forces based only on the maximum runup height, which can be obtained directly from inundation maps. This approach was taken partly because no other data and information were readily available. Based on FEMA P646, the American Society of Civil Engineers has substantially revised and expanded its previous version (ASCE/SEI 7-10) for the chapter dealing with tsunami loads and their effects on buildings and other structures. This new standard
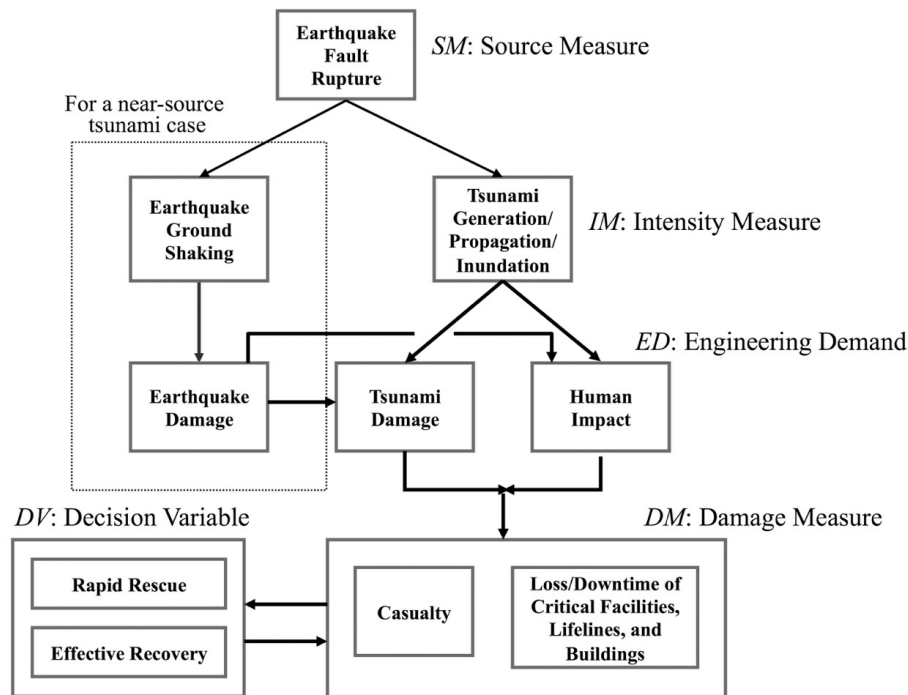
Fig. 2. Conceptual view of a comprehensive source-to-end scenario- and performance-based analysis.

will be included in Chapter 6 of ASCE/SEI 7-16 [22], and requires site-specific probabilistic hazard analysis for essential structures in tsunami-danger zones, running a numerical simulation from the source to match the pre-established probabilistic offshore tsunami amplitude.

3. Data Explorer

Tsunami analysis requires a comprehensive local investigation, where we study a specific individual object at a specific location. **Fig. 2** presents a conceptual view of this kind of performance-based tsunami assessment. The current PTHA method provides the first two initial stages in **Fig. 2**: source measure (SM) and intensity measure (IM) of tsunami hazard. To determine the effects of tsunami flow on a structure, an accurate location must be known, as well as the flow paths of the tsunami inundation processes. A tsunami's hydrodynamic forces (including debris effects) could be quite different near neighboring structures due to local flow interactions with surrounding features (as demonstrated in **Fig. 1**). Given the importance of this spatial context, a GIS-based platform was key to the development of a tsunami flow data query tool. The Data Explorer, introduced here, is a tool that represents a unique attempt at conducting a comprehensive analysis of performance-based tsunami assessment for any location. It facilitates the evaluation of engineering demand (ED) and damage measure (DM) for an object of interest (such as a structure or facility). The ED and DM components are critical for conducting a source-to-end performance-based analysis, as laid out in **Fig. 2**.

The Data Explorer's web-based interface (**Fig. 3**) allows engineers to interactively query large tsunami sim-

ulation datasets for specific locales. For a given location of interest, time-series data from tsunami simulations are collected and stored at fine-scale temporal and spatial resolutions. These data can represent the outcomes of probabilistic tsunami hazard assessment (PTHA) with uncertainty quantification. The tool presents temporal data representing flow velocity and inundation depth at each grid point (approximately 10 m resolution) across the entire modeled region. In other words, the Data Explorer allows users to obtain tsunami flow depth and velocity data directly from the simulations, instead of estimating those values from the parameter of the maximum runup height for an event. In this manner, users can quickly extract tsunami flow data from any point within the extent of the simulation, and analyze the tsunami effects (i.e., forces on structures across the time series of the simulated event).

The concepts underlying the Data Explorer are not new and are considered a "best attainable" approach for tsunami hazard analysis at the present time. In practice, however, full implementation of the concepts represents a formidable challenge. For example, let us consider the ASCE/SEI 7-16 requirement for the evaluation of essential coastal structures, which requires running a complete numerical inundation model matching the defined probabilistic offshore tsunami conditions specified with the parameters (i.e. offshore tsunami amplitude and effective wave period). Significant effort and computing resources are required to accomplish this task, even for a single case of a probabilistic tsunami event.

Rather than incurring the resource costs to run a numerical simulation for each specific site of interest, the Data Explorer aggregates the outputs generated by numerical simulations of multiple possible tsunami scenarios. The data calculated at every grid point and every time step in
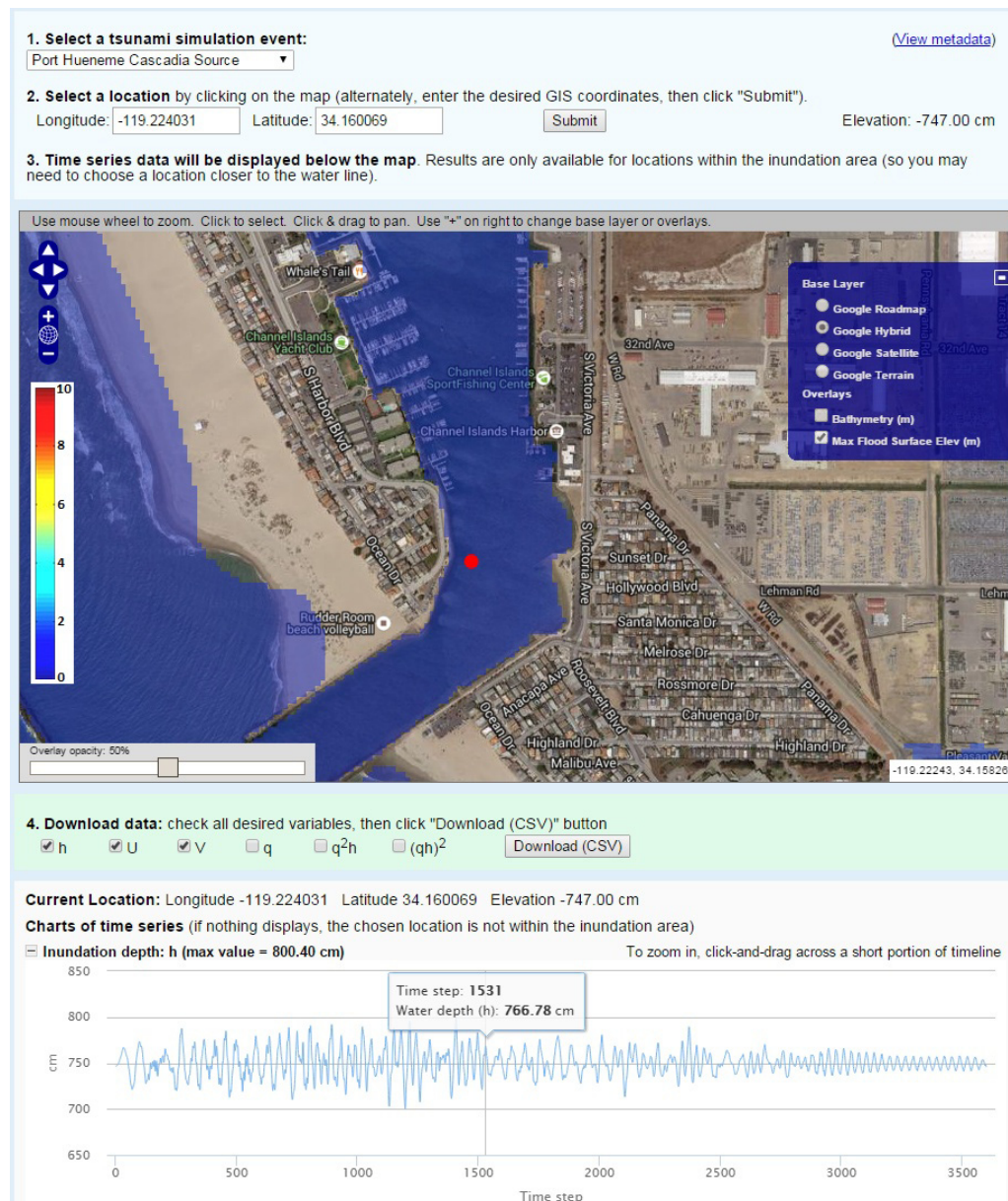
Fig. 3. The data explorer interface.

the entire region (typically several square km of a coastal area) by each simulation are gathered and stored. This allows the Data Explorer to retrieve the complete time series (data representing water depth and flow velocities) of an event at a selected location, delivering the data extremely quickly and conveniently in the format necessary for in-depth analysis. With the extracted data at hand, the user can then compute the hydrodynamic forces, moments, buoyancy forces, scour effects, etc. The availability of datasets representing a wide range of probabilistic tsunami scenarios, together with extremely fast retrieval of the high-resolution data, result in an effective tool for helping to calculate the quantitative uncertainty analysis associated with spatial and temporal variability.

To use the Data Explorer, the user first selects an area of the coastline and a specific tsunami source event. The event can be a true historical event or a synthesized probabilistic tsunami event, selected from the events stored in the portal. Bathymetry and topography data for the area are loaded, as well as metadata for the selected event and backend connections to the large simulation output data files (grids). Once the event is selected and loaded, the user can manually enter the latitude and longitude of a desired location to set the point of interest, or browse locations using the interactive map. Typical zooming and panning capabilities are provided, and the map incorporates standard Google Maps base layers, bathymetry for the area, and a layer representing maximum flood surface elevation.

The user can explore the effects of inundation interactively by clicking on the map to set points of interest at the locations of specific structures: for example, pilings
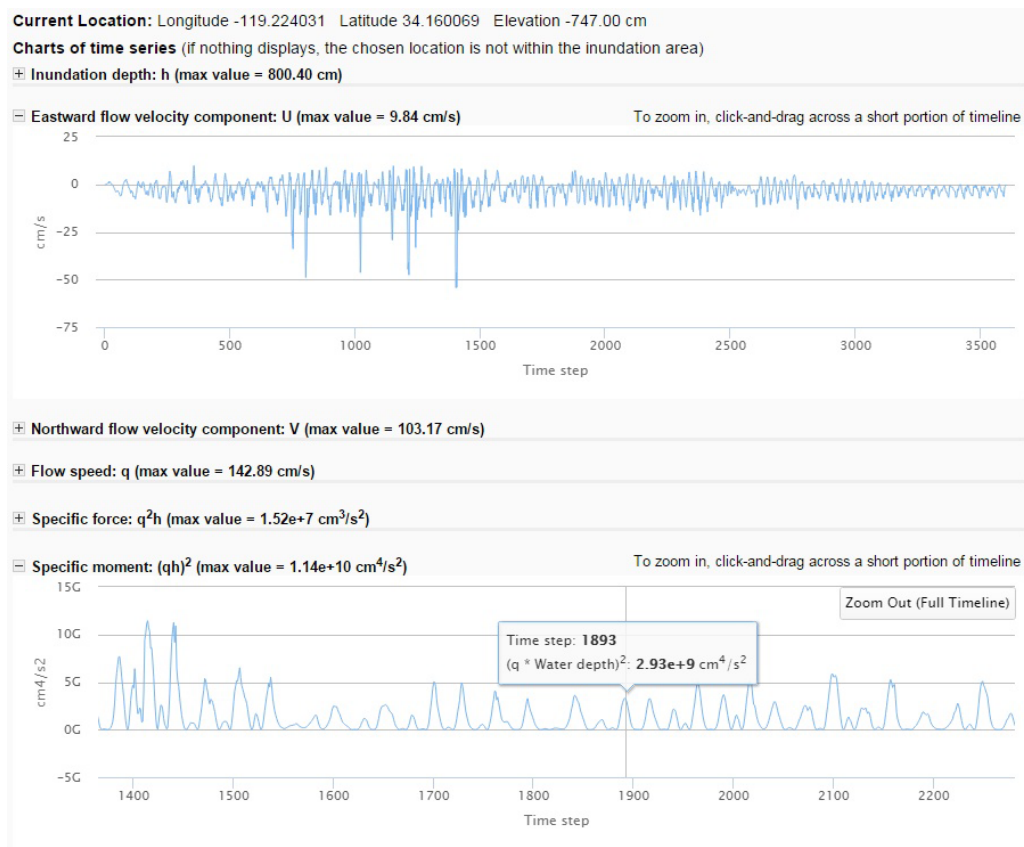
Fig. 4. Charts calculated on the fly from time series data extracted at the map point selected by the user. Two are expanded in this view, and the "Specific moment" has been zoomed-in to provide more detail.

or the concrete footings of a bridge. The tool quickly (in less than a second) extracts a time series of the tsunami inundation data (flow velocities and depth) at the selected location by indexing into the output grids across thousands of time steps. Commonly used parameters for structural analysis (such as maximum specific force, maximum overturning moment, etc.) are calculated by the system and represented in interactive charts. The specific force is defined as q^2h where q is the flow speed and h is the flow depth. This parameter is part of the hydrodynamic force acting on an object ($\frac{1}{2}\rho c_d B(hq^2)$ where B is the breadth of the object, c_d is the resistance coefficient, and ρ is the fluid density). Overturning moment is the product of the force and the moment arm (i.e., 0.5 h); therefore, it is calculated here as q^2h^2. The actual moment can be computed by $\frac{1}{4}\rho c_d B(h^2q^2)$.

The user can view the results in six zoomable charts (**Fig. 4**) and interactively move the cursor across them to display individual data values, making it possible to quickly identify how and where conditions change for engineering sensitivity analysis. The charts can be collapsed or expanded individually to display only those of primary interest. The maximum value of each parameter is always displayed, allowing the user to quickly explore different points on the map and see exactly how the maximum inundation depth and associated values change along a structure or flow path.

A temporal view of tsunami inundation and associated wave data is necessary for calculating wave and related forces. The Data Explorer's web-based GIS platform is capable of instantaneously providing the critical time series data (flow velocities and depth) of tsunami inundation. With this information, we can directly calculate the necessary parameters for structural analysis: namely, the maximum specific force (a.k.a. momentum flux), Max (hq^2), and the maximum overturning moment Max (h^2q^2). Further, the time history of flow conditions allows us to estimate impact forces of floating debris, as well as buoyancy forces and scour effects [7]. Quick access to the time-series data in this direct fashion makes it possible to analyze many hazard scenarios, important since each scenario has some probability of occurrence. To facilitate the comparison of results at different locations and/or from different scenarios, the forces can also be downloaded (in CSV format) and stored for further analysis.

4. Data Handling and Computing Infrastructure

The tsunami simulation output data available in the Data Explorer were generated by researchers using a computational tsunami simulation model, with the source conditions modified for each run. As output, the simulation model code produced a volumetric block of data for each tsunami variable of interest: h (wave amplitude), U (east-

ward) and V (northward) velocities. Each data volume represents an (i, j) 2-dimensional location and time index t, packaged in NetCDF format.

The data were transformed from NetCDF to BIP (Band Interleaved by Pixel) to maximize data retrieval efficiency. NetCDF files are hierarchically-organized data structures capable of describing a variety of multidimensional datasets. This data-structuring generality is beneficial in many scenarios, but also has the downside of increasing the computational overhead required to extract information. By organizing the data in a specific binary structure, the time series data is arranged contiguously on disk, and a simple file reader (a custom 20-line C program) can be used to extract an entire time series group of data values at any arbitrary (i, j) location (within a predefined extent). This resulted in significantly faster retrieval times, and gives the user nearly instantaneous response to each map click.

Data conversion from NetCDF to BIP was performed via the open source raster manipulation library GDAL [24] – specifically, the gdal_translate utility – with a NetCDF extension compiled into it. Using particular command-line switches, the gdal_translate utility restructured each file accordingly.

When the user clicks within the constrained extent of the interface map to retrieve time series data at a point, an event is generated and client-side JavaScript code captures the X/Y location of the mouse click within the local rectangular coordinate space. The X/Y coordinates are then sent via an asynchronous connection to server side middleware that, knowing the extent of the current map view, converts the X/Y coordinates to (i, j) rectangular coordinates of the data array. The tsunami simulation output data is stored as large BIP grids on a central NAS (networked attached storage) device. A Linux-based processing server handles incoming requests generated by map clicks, indexing into the BIP grids via the converted (i, j) array coordinates to extract time series data at that point. The results are returned to the middleware code, which then translates the resulting time series data values to JSON (JavaScript Object Notation) text and passes them back to the web client.

The JSON text received by the client contains three time series data blocks (h, U, and V) for all time steps at the (i, j) location where the user clicked on the map. These time series data blocks are then used to calculate the parameters q ($= \sqrt{U^2 + V^2}$), q^2h and $(qh)^2$. Maximum values across the time series for each of the six variables are determined on the client and printed alongside each chart title below the map. If a variable's graph is visible (expanded), a line graph of the data is rendered via the HighCharts [25] JavaScript library. The open source OpenLayers [26] JavaScript library and MapServer [27] software are used to generate the map and overlay the available spatial layers, as well as capturing mouse clicks and translating the pixel values into projected coordinate values. The jQuery [28] JavaScript library handles the DOM (Document Object Model) manipulation and asynchronous calls to the server to retrieve time series data.
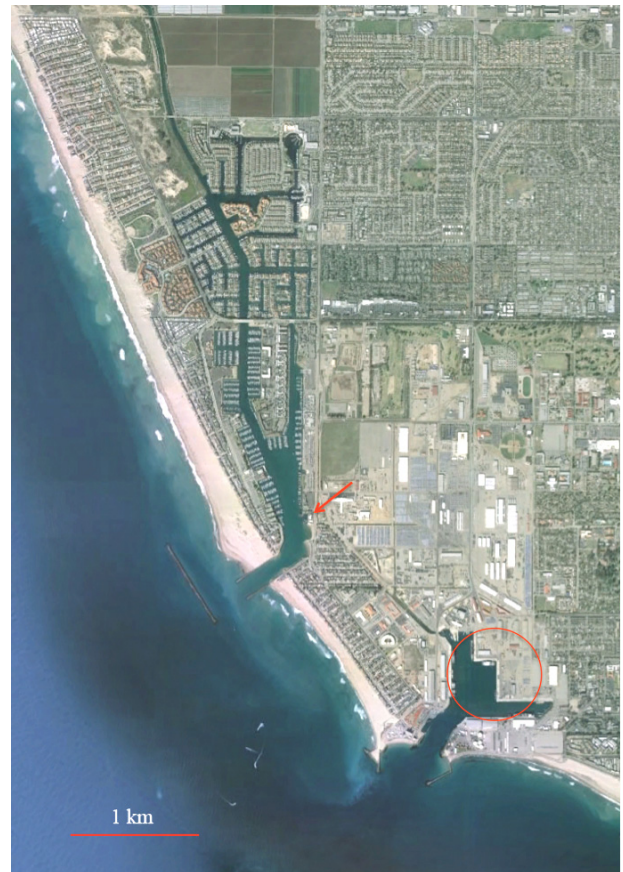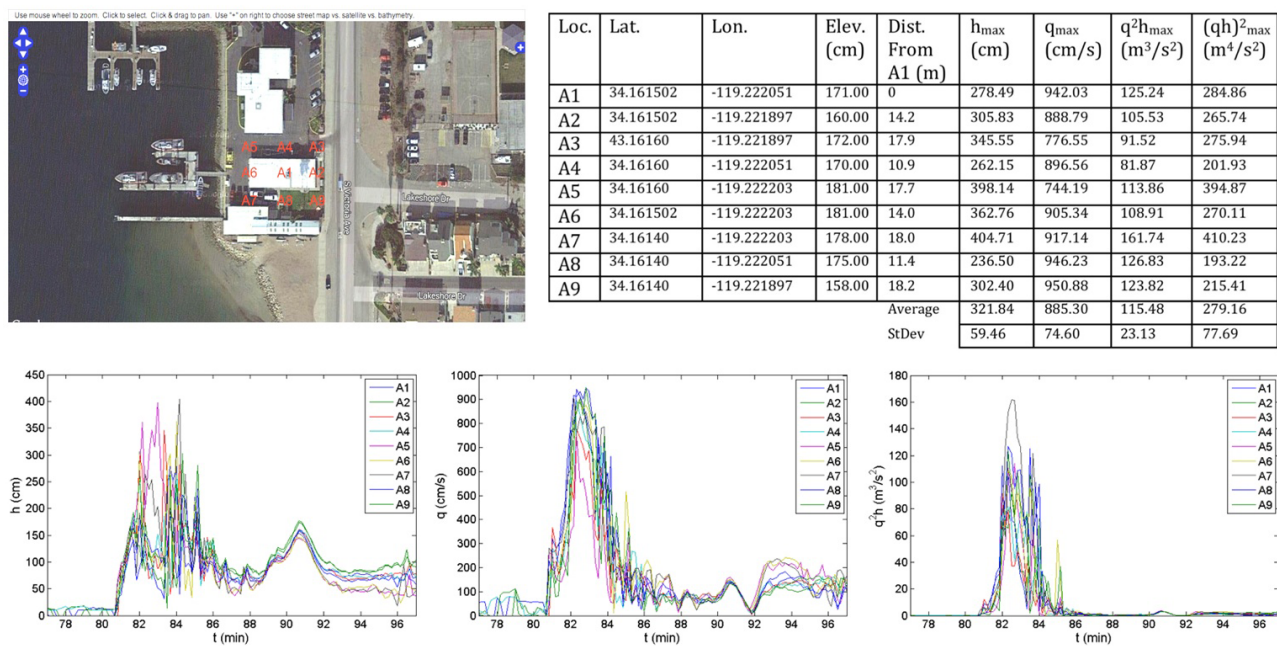

Fig. 5. The domain of interest for the two Data Explorer example scenarios. The location of Example 1 (building analysis) is shown by the red arrow. The location of Example 2 (quay wall analysis) is shown by the red circle.

5. Example Scenarios

The two examples provided in this section are located as marked in **Fig. 5**. The first example demonstrates how the Data Explorer can be used to extract tsunami flow data for multiple point locations around the building indicated by a red arrow in the figure. As shown in **Fig. 6**, nine adjacent locations (A1-A9) representing the center, sides, and corners of the building were selected and then used to quantify uncertainties associated with the numerical simulation for a given tsunami event. For each point, the Data Explorer returned time series data representing inundation depth, eastward flow velocity, northward flow velocity, flow speed, specific force, and specific moment, as well as the maximum value of each parameter for the selected event. The three time-series plots of **Fig. 6** show the inundation depths (left), flow speeds (middle) and specific forces (right). It is remarkable to find substantial variability in the data from a single numerical simulation around a relatively small building (approximately 10 × 30 m).

Using the retrieved data, we can calculate estimated forces, moments, scour effects, and other parameters of interest. In order to conduct a complete probabilistic analysis, the process described in this example would be repeated for other tsunami scenarios, including synthesized

Loc. table and figures:

Loc.	Lat.	Lon.	Elev. (cm)	Dist. From A1 (m)	h_{max} (cm)	q_{max} (cm/s)	q^2h_{max} (m³/s²)	$(qh)^2_{max}$ (m⁴/s²)
A1	34.161502	-119.222051	171.00	0	278.49	942.03	125.24	284.86
A2	34.161502	-119.221897	160.00	14.2	305.83	888.79	105.53	265.74
A3	43.16160	-119.221897	172.00	17.9	345.55	776.55	91.52	275.94
A4	34.16160	-119.222051	170.00	10.9	262.15	896.56	81.87	201.93
A5	34.16160	-119.222203	181.00	17.7	398.14	744.19	113.86	394.87
A6	34.161502	-119.222203	181.00	14.0	362.76	905.34	108.91	270.11
A7	34.16140	-119.222203	178.00	18.0	404.71	917.14	161.74	410.23
A8	34.16140	-119.222051	175.00	11.4	236.50	946.23	126.83	193.22
A9	34.16140	-119.221897	158.00	18.2	302.40	950.88	123.82	215.41
				Average	321.84	885.30	115.48	279.16
				StDev	59.46	74.60	23.13	77.69

Fig. 6. Quantification of uncertainties using the Data Explorer for the building indicated in **Fig. 5**. The user identifies locations of interest (nine locations A1-A9 were selected here), then compares the maximum values of relevant parameters returned for each location, along with the time series data, which can be graphed collectively. The plots here represent inundation depth (left), flow speed (middle), and specific force (right).
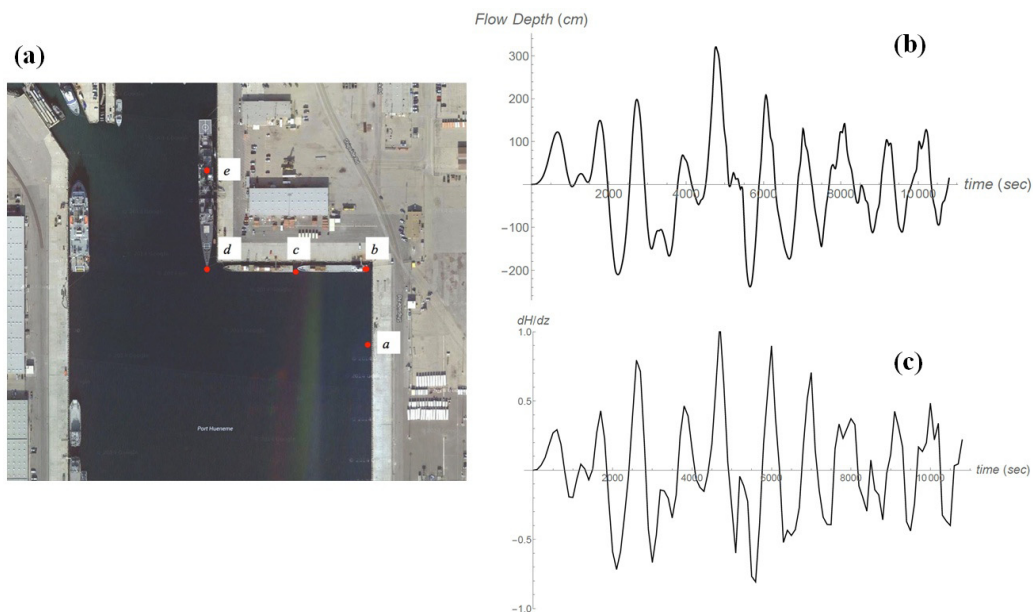
Fig. 7. Quantification of uncertainties using the Data Explorer for the quay wall of the port shown in **Fig. 5**. This figure displays: (a) The locations of interest (five locations $a - e$ are selected here); (b) the retrieved time-series data of the water-surface elevation at the location a; (c) the computed pore-water-pressure gradient at $z = 0$.

probabilistic tsunami hazards. The results would then be aggregated to produce the probabilistic outcome with uncertainty that can be verified against the data.

The second example demonstrates the evaluation of potential quay wall failures due to momentary liquefaction caused by a tsunami's rapid drawdown [29]. The location of the port facility is shown as a red circle in **Fig. 5**. Five different points along the quay wall were selected

(**Fig. 7a**), and data were retrieved at each of the five points across four different tsunami scenarios. **Fig. 7b** shows the time series data representing tsunami inundation depth at Location a. This operation is fast and easy to conduct in the Data Explorer. With the obtained inundation data, the vertical gradients of pore-water-pressure head $\partial H/\partial z$ (the coordinate z points vertically upward) are then calculated to seek the occurrence of momentary liquefaction

Table 1. Summary of soil instability analysis at the five locations along the quay wall for four scenario tsunami cases. We use the instability criterion assuming that momentary soil liquefaction will be induced when the pore-water-pressure gradient becomes $\partial H/\partial z < -0.5$ [30].

Tsunami Scenarios	Locations	Max. WS EL (cm)	Min. WS EL (cm)	Min. $\partial H/\partial z$	depth (cm) of $\partial H/\partial z < -0.5$
AK	a	312.7	-237.9	-0.807	-209.6
AK	b	323.9	-231.7	-0.794	-189.8
AK	c	328.5	-236.2	-0.741	-77.4
AK	d	323.7	-252.8	-0.797	-93.7
AK	e	340.8	-260.5	-0.783	-86.8
CAS	a	33.8	-41.7	-0.206	0.0
CAS	b	35.1	-33.7	-0.134	0.0
CAS	c	34.5	-33.8	-0.146	0.0
CAS	d	38.3	-37.4	-0.216	0.0
CAS	e	37.9	-36.8	-0.130	0.0
CH	a	206.2	-225.7	-0.628	-95.3
CH	b	210.1	-235.8	-0.584	-68.5
CH	c	210.7	-229.7	-0.641	-96.9
Ch	d	211.0	-230.6	-0.619	-85.2
Ch	e	204.6	-230.3	-0.636	-88.7
JP	a	58.2	-80.3	-0.282	0.0
JP	b	59.1	-81.0	-0.281	0.0
JP	c	58.6	-80.8	-0.281	0.0
JP	d	59.1	-80.8	-0.287	0.0
JP	e	59.6	-81.5	-0.288	0.0

based on the method developed by Yeh and Mason [30]. Total liquefaction is considered to occur when the condition $\partial H/\partial z < 1 - \rho_{sat}/\rho \approx -0.93$ is reached, assuming sandy soils [29, 30]. This is the condition where the pore-water pressure gradient reaches the level of the buoyant specific weight of the saturated soil skeleton. According to [29], however, severe soil instability is anticipated much earlier, say $\partial H/\partial z < 1 - \rho_{sat}/\rho \approx -0.5$, because of the presence of flows and other disturbance. **Fig. 7c** shows the time series of $\partial H/\partial z$ at $z = 0$. Although no total liquefaction is anticipated at Location a, the values of pore-water-pressure gradient become less than -0.5 several times, indicating instability.

With the use of the method to estimate pore-water-pressure gradients in soils [30], the deepest penetration depths of the condition $\partial H/\partial z < -0.5$ for all five points ($a - e$ in **Fig. 7a**) were then calculated and are presented in **Table 1**. The results indicate that two of the four scenarios may cause soil instability that could potentially induce the quay wall failure. The worst condition occurs at the different locations: -209.6 cm at Location a for the scenario AK and -96.9 cm at Location c for Scenario CAS.

The foregoing analysis of the predictions and uncertainty estimates for soil instability were made in just a few hours using a web browser and spreadsheet. The functionality and performance of the Data Explorer provide an extremely convenient and effective tool for engineers to conduct performance-based tsunami engineering analysis together with the quantification of uncertainties based on the data.

6. Conclusions

The Data Explorer represents an effective tool for the analysis of critical coastal structures that require probabilistic considerations with regard to uncertainty quantification. Significant advances in information technology – in particular, computational speed, data handling, and the ability to store massive datasets and quickly index through them – have facilitated the development of this tool. The Data Explorer can be used to evaluate quantifiable uncertainty supported by the data for a given critical structure. In spite of the presence of substantial uncertainty in tsunami hazard estimates, this tool enables users to comprehensively analyze a structure using the best available engineering models and knowledge, minimizing potentially unreliable expert judgment and guesswork.

Further development of the Data Explorer is planned, including the ability to automate the calculation of additional parameters and the production of additional charts and graphs, as well as the ability to define multiple points of interest in the interface itself and download a spreadsheet containing all simulated and calculated data for all points.

References:
[1] H. Yeh, S. Sato, and Y. Tajima, "The 11 March 2011 East Japan Earthquake and Tsunami: Tsunami Effects on Coastal Infrastructure and Buildings," Pure Appl. Geophys., Vol.170, pp. 1019-1031, 2013.
[2] F. Kato, Y. Suwa, K. Watanabe, and S. Hatogai, "Damages to Shore Protection Facilities Induced by the Great East Japan Earthquake Tsunami," J. of Disaster Research, Vol.8, No.4, pp. 612-625, 2013.
[3] Building Research Institute, "Quick Report of the Field Survey and Research on "The 2011 off the Pacific coast of Tohoku Earthquake" (the Great East Japan Earthquake)" Technical Note, National Institute fro Land and Infrastructure Management, No.636, 2011.
[4] K. Konagai, T. Kiyota, and H. Kyokawa, "Piles for RC/Steel-frame buildings pulled up by tsunami at Onagawa Town, in the March 11th 2011 East Japan Earthquake," Quick Report of Recon. No.2 Konagai/Kiyota Laboratories, IIS, University of Tokyo, Vol.9, 2011.
[5] K. Hayashi, S. Tamura, M. Nakashima, Y. L. Chung, and K. Hoki, "Evaluation of Tsunami Load and Building Damage Mechanism Observation in the 2011 off Pacific Coast of Tohoku Earthquake," 15th World Conference on Earthquake Engineering, Paper ID 1807, Sep., 2012.
[6] American Nuclear Society, "Fukushima Daiichi: ANS Committee Report," 2012, available online at http://fukushima.ans.org/report /cleanup [accessed Dec. 15 2015]
[7] H. Yeh, A. R. Barbosa, H. Ko, and J. G. Cawley, "Tsunami loadings on structures: Review and analysis," Proceedings of 34th Conference on Coastal Engineering, Seoul, Korea, 2014.
[8] D. Keon, C. M. Pancake, and H. Yeh, "Protecting Our Shorelines: Modeling the Effects of Tsunamis and Storm Waves," Computer 11, pp. 23-32, 2015.
[9] H. Yeh, "Tsunami Hazard and Casualty Estimation Model," Tenth US National Conf. on Earthquake Engineering, 2014.
[10] N. Shuto N and K. Fujima, "A Short History of Tsunami Research and Countermeasures in Japan," Proc. of the Japan Academy Series B, Physical and Biological Sciences, Vol.85, No.8, pp. 267-275, 2009.

[11] L. G. Geist and T. Parsons, "Probabilistic Analysis of Tsunami Hazards," Natural Hazards, Vol.37, pp. 277-314, 2006.

[12] H. K. Thio, P. Somerville, and G. Ichinose, "Probabilistic Analysis of Strong Ground Motion and Tsunami Hazards in Southeast Asia," J. of Earthquake and Tsunami, Vol.1, No.2, pp. 119-137, 2007.

[13] F. I. González, E. L. Geist, B. E. Jaffe, U. Kanoglu, H. O. Mofjeld, C. E. Synolakis, V. V. Titov, D. Arcas, D. Bellomo, D. Carlton, T. Horning, J. Johnson, J. Newman, T. Parsons, R. Peters, C. Peterson, G. Priest, A Venturato, J. Weber, F. Wong, and A. Yalciner, "Probabilistic Tsunami Hazard Assessment at Seaside, Oregon, for Near- and Far-field Seismic Sources," J. of Geophysical Research: Oceans, 114-C11, 2009.

[14] F. I. González, R. J. LeVeque, and L. M. Adams, "Probabilistic Tsunami Hazard Assessment (PTHA) for Crescent City, CA. Final Report for Phase I," University of Washington Department of Applied Mathmatics, 2013.

[15] E. L. Geist and P. J. Lynett, "Source Processes for the Probabilistic Assessment of Tsunami Hazards," Oceanography, Vol.27, No.2, pp. 86-93, 2014.

[16] C. A. Cornell, "Engineering Seismic Risk Analysis." Bulletin of the Seismological Society of America, Vol.58, pp. 1583-1606, 1968.

[17] NRC (National Research Council), "Probabilistic Seismic Hazard Analysis," National Academy Press, Washington, D.C., 1988.

[18] L. M. Adams, R. J. LeVeque, and F. I. González, "The Pattern Method for Incorporating Tidal Uncertainty into Probabilistic Tsunami Hazard Assessment (PTHA)," Natural Hazards, Vol.76, No.1, pp. 19-39, 2015.

[19] FEMA P646, "Guidelines for Design of Structures for Vertical Evacuation from Tsunamis," Federal Emergency Management Agency, Washington, D.C., 2008, available online at https://www.fema.gov/media-library/assets/documents/14708 [accessed Dec. 15 2015]

[20] S. Koshimura, Y. Namegaya, and H. Yanagisawa, "Tsunami Fragility: A New Measure to Identify Tsunami Damage," J. of Disaster Research, Vol.4, No.6, pp. 479-488, 2009.

[21] C. A. Kircher and J. Bouabid, "New Building Damage and Loss Functions for Tsunami," Tenth U.S. National Conference on Earthquake Engineering, 2014, available online at https://nees.org/resources/11302/download/10NCEE-000322.pdf [accessed Dec. 15 2015]

[22] American Society of Civil Engineers ASCE/SEI 7-16, Minimum Design Loads for Buildings and Other Structures, 2016, available online at http://standards.plantops.umich.edu/ascesei-7-16-design-loads-for-buildings [accessed Apr. 29, 2016]

[23] H. Yeh, A. Barbosa, H. Ko, and J. Cawley, "Tsunami Loadings on Structures: Review and Analysis," Proc. of 34th Conf. of Coastal Engineering, Seoul, South Korea, 2015.

[24] GDAL open source library, available online at http://www.gdal.org [accessed Dec. 27 2015]

[25] HighCharts JavaScript charting library, available online at http://www.highcharts.com [accessed Dec. 17, 2015]

[26] OpenLayers open source JavaScript mapping library, available online at http://www.openlayers.org [accessed Dec. 17, 2015]

[27] MapServer open source web-mapping development environment, available online at http://www.mapserver.org [accessed Dec. 17, 2015]

[28] jQuery cross-platform JavaScript library, available online at http://www.jquery.com [accessed Dec. 17, 2015]

[29] S. Tonkin, H. Yeh, F. Kato, and S. Sato, "Tsunami scour around a cylinder," J. of Fluid Mechanics, Vol.496, pp. 165-192, 2003.

[30] H. Yeh and H. B. Mason, "Sediment response to tsunami loading: Mechanisms and estimates," Géotechnique, Vol.64 No.2, pp. 131-143, 2014.

Name:
Dylan Keon

Affiliation:
Associate Director, Northwest Alliance for Computational Science and Engineering, Oregon State University

Address:
2007 Kelley Engineering Center, Oregon State University, Corvallis, OR 97331, USA
Brief Career:
1994-1997 USGS Biological Resources Division
1997-2000 Department of Botany and Plant Pathology, Oregon State University
2000-present Northwest Alliance for Computational Science and Engineering, Oregon State University
Selected Publications:
● "Web-based spatiotemporal simulation modeling and visualization of tsunami inundation and potential human response," Int. J. of Geographic Information Science, Vol.28 No.5, pp. 987-1009, 2014.
● "Protecting Our Shorelines: Modeling the Effects of Tsunamis and Storm Waves," IEEE Computer, pp. 23-32, Nov, 2015.
Academic Societies & Scientific Organizations:
● Association of American Geographers (AAG)

Name:
Cherri M. Pancake

Affiliation:
Professor Emeritus, Electrical Engineering and Computer Science, Oregon State University

Address:
2027 Kelley Engineering Center, Oregon State University, Corvallis, OR 97331, USA
Brief Career:
1986-1992 Assistant Prof., Computer Science and Engineering, Auburn University
1992-2015 Assoc Prof. and Professor of EECS, Oregon State University
2015-present Director, Northwest Alliance for Computational Science and Engineering
Selected Publications:
● "Protecting Our Shorelines: Modeling the Effects of Tsunamis and Storm Waves," IEEE Computer, pp. 23-32, Nov, 2015.
Academic Societies & Scientific Organizations:
● Association for Computing Machinery (ACM), Fellow
● Institute of Electrical & Electronics Engineers (IEEE), Fellow
● ACM Special Interest Group on High Performance Computing (SIGHPC), Chair

Name:
Ben Steinberg

Affiliation:
Software Research Engineer, Northwest Alliance for Computational Science and Engineering, Oregon State University

Address:
2017 Kelley Engineering Center, Oregon State University, Corvallis, OR 97331, USA

Brief Career:
1996- Research Assistant, Partnership for Research In Stereo Modeling (PRISM), Department of Computer Science, Arizona State University
1999- Systems Programmer, Arizona State University Mars Space Flight Facility
2005 Joined the Northwest Alliance for Computational Science and Engineering at Oregon State University

Name:
Harry Yeh

Affiliation:
Professor, School of Civil and Construction Engineering, Oregon State University

Address:
101 Kearney Hall, Oregon State University, Corvallis, OR 97331, USA

Brief Career:
1977-1983 Hydraulic Engineer, Bechtel Inc., San Francisco, CA
1983-2002 Assistant, Associate, and Full Professor, University of Washington
2003-present Professor, Oregon State University

Selected Publications:
● "Laboratory Experiments on Counter-Propagating Collisions of Solitary Waves. Part 1: Wave Interactions & Part 2: Flow Field," J. Fluid Mech., Vol.749, 577-596.1 & 755, pp. 463-484.
● "On the Mach Reflection of a Solitary Wave – Revisited," J. Fluid Mech., Vol.672, pp. 326-357.
● "Sediment Response to Tsunami Loading: Mechanisms and Estimates," Géotechnique, Vol.64, No.2, pp. 131-143.
● "Feature Surfaces in Symmetric Tensor Fields Based on Eigenvalue Manifold," IEEE TVCG, Vol.22, No.3, pp. 1248-1260.

Academic Societies & Scientific Organizations:
● American Society of Civil Engineering (ASCE)
● American Geophysical Union (AGU)
● Earthquake Engineering Research Institute (EERI)